EFFECT OF NITROGEN PARTIAL PRESSURE ON REACTIVE MAGNETRON SPUTTERING FROM $Ti_{13}Cu_{87}$ METALLOID TARGET: SIMULATION OF CHEMICAL COMPOSITION

A. RAHMATI, M. KHANZADEH

Faculty of Science, Vali-e-Asr University of Rafsanjan
(Rafsanjan, Iran; e-mail: a.rahmati@vru.ac.ir)

UDC 539.2

A sintered $Ti_{13}Cu_{87}$ composite target was reactively sputtered in Ar–N_2 gas mixtures, and sputtered species were deposited on Si (111) substrates. We study the pressure-dependent target mode variation of the $Ti_{13}Cu_{87}$–N_2 system, by measuring the N_2 partial pressure, deposition rate, target voltage, and Ti and Cu concentrations for various reactive N_2 gas flow ratios. The $Ti_{13}Cu_{87}$ target surface begins to be nitrided with increasing N_2 flow ratio, which is caused by the absorption and the implantation of N_2 gas on the $Ti_{13}Cu_{87}$ target surface. Hence, the deposition rate was reduced due to the lower sputtering yield and a higher scattering under the mass transport between the target-substrate spacing. Secondary electron emission yield of the nitride portion of target surface is higher than that of the unnitrided portion. Therefore, at a constant sputtering power, the target voltage decreases, as the N_2 partial pressure increases. By means of the TRIM.SP Monte-Carlo simulation, the particle reflection coefficients of reflected neutrals was calculated. The initial energies of reflected neutrals and the sputtered particles at the substrate were estimated using the simple binary collision model and the distribution-weighted averages, respectively. Their final energies depend on the energy dissipation during the mass transport through the gas phase. The energy and angular characteristics of the sputtering yield were extracted from the available literature to obtain a prediction about a final composition of films.

1. Introduction

When applying, for example, the pulsed laser deposition or magnetron sputtering to grow multicomponent thin films, a multielemental material source is used to avoid the loss of compositional control. In the latter case, it is clear that this approach does not guarantee the compositional control due to the transport of sputtered particles through the sputter gas and the preferential sputtering by energetic particles during the thin film deposition. Nevertheless, this technique is vastly used in the industrial era. A simulation strategy may give an interesting perspective to control and to predict the composition of complex thin films.

Reactive magnetron sputtering methods have been widely used to form compound thin films [1–3]. As usual, the formation of a compound layer on the surface of a metal target (i.e. compound mode) is closely related to the deposition of a compound thin film. Therefore, sputtering parameters such as the partial pressure of a reactive gas and the sputtering power are carefully controlled to maintain the target surface in an appropriate state [4–7].

In the present study, the pressure-dependent target mode variation of the $Ti_{13}Cu_{87}$–N_2 system is investigated by measuring the N_2 partial pressure, deposition rate, target voltage, and Ti and Cu concentrations for various reactive N_2 gas flow ratios.

2. Methods

2.1. Experiments

A sintered Ti–Cu composite target (13 at. %Ti, 76 mm in diameter and 4.5 mm in thickness) was reactively sputtered in the Ar/ N_2 gas mixture, and sputtered species were condensed on ultrasonically precleaned Si (111) substrates. The working chamber of the sputtering system was pumped down via a rotary pump and a turbomolecular pump allowing a base pressure of less than 1.5×10^{-3} Pa to be maintained. The distance between the substrate and the target was fixed at 19.5 cm. The argon and nitrogen flow rates regulated by MKS flowmeters were adjusted at $Q_{\mathrm{Ar}} = 25$ and $Q_{\mathrm{N2}} = 0$–22 sccm, respectively. Under these deposition conditions, the total pressure varied between 0.12–0.82 Pa, and the substrate temperature and the sputtering power were close to 150 °C and 200 W, respectively.

The chemical composition of the films was determined using an energy dispersive X-ray spectrometer coupled with a scanning electron microscope (SEM/EDX, Philips XL30). The mass of deposited films was measured by a Sartorius balance with 10^{-5} g certainty. The films'

deposition rate (R) was calculated as

$$R = \frac{\Delta m}{\rho S t}, \tag{1}$$

Δm and ρ are the mass and the density of a deposited film, respectively; S and t are film's cross section area (2×0.5 cm^2) and the deposition time, respectively.

2.2. Simulations and Models

2.2.1. Reflected particles and their energy

The particle reflection coefficient is defined as a fraction of the impinging ion flux on the target that reflected. It is estimated using the TRIM.SP Monte-Carlo simulation [8]. The flux density of arrived N neutrals on the substrate is determined by the flux density of reflected N neutrals from the target and the relative area of the substrate $A^{\rm s}$ to a racetrack on the target $A^{\rm t}$.

Wang *et al.* [9] proposed that the energetic N's are generated from N_2^+ ions after these ions are accelerated through the (cathode) sheath and are dissociatively reflected from the cathode. The energy reflection coefficient (R_E) is given by the energy of reflected neutral N's per that of impinging ions. The energy of impinging ions is only 0.75 of the discharge voltage, eV_d [10]. Using a simple binary collision model (collision between N and each component of target, i.e. Ti and Cu atoms), which predicts that the ratio of the reflected energy ($E_{\rm ref}$) and the energy of impinging ions ($0.75eV_d$) is determined by each target's component mass ($M_{\rm Ti}$ and $M_{\rm Cu}$), target composition, and N atom mass ($M_{\rm N}$):

$$R_E^i = \frac{E_{\rm ref}^i}{0.75eV_d} \approx f\sum_{j=1}^{2} c_j \frac{M_j - M_i}{M_j + M_i}, \qquad i = {\rm Ar, N}, \tag{2}$$

where c_j is the mole fraction of each component, and j = Ti, Cu. The factor f on the right-hand side of Eq. (2) is one for the Ar reflection. But this factor is 0.5 for the N reflection, N_2^+ collision with the cathode resembles that of two N atoms colliding with the cathode independently with the half of N_2^+ initial energy.

2.2.2. Simulation of the sputtering process

The sputtering yield depends on the energy and the angular distribution such as

$$Y(E,\theta) = Y(E)S(\theta), \tag{3}$$

where E is the energy of incident ions, and θ is the ejection angle of sputtered atoms with respect to the surface normal. The energy dependent part was calculated by the semiempirical formula [11]

$$Y(E) = qs_n^{\rm KrC}(\varepsilon)\frac{\left(\frac{E}{E_{\rm th}}-1\right)^{\mu}}{\lambda + \left(\frac{E}{E_{\rm th}}-1\right)^{\mu}}, \tag{4}$$

where q, $E_{\rm th}$, μ and λ are material-dependent parameters listed in the Table 1 for pairs of an incident ion and a target atom. The quantities $E_{\rm th}$ and $s_n^{\rm KrC}(\varepsilon)$ are the threshold energy for sputtering and the nuclear stopping power, respectively.

The angular distribution of sputtered atoms with the heart shape was proposed by Yamamura *et al.* [12] as

$$S(\theta) = \cos\theta(1 + B\cos^2\theta), \tag{5}$$

where B is a fitting parameter. The fitting parameter depends on the mass and the binding energy of a target material and the mass and the energy of ions. It can be expressed as

$$B = B'{\rm Ln}Q - B_c' \quad \text{and} \quad Q = \frac{M_t E}{M_g E_{\rm sb}}, \tag{6}$$

where M_t is the mass of the sputtered atom, $E_{\rm sb}$ is the binding energy of the sputtered material (Table 1). The values of B' and B_c' were respectively approximated as 0.488 and 2.44.

2.2.3. Simulation of the film composition

A rough estimation of the atomic Ti:Cu ratio in films is given by

$$\begin{aligned}{\rm Ti:Cu} = \frac{c_b^{\rm Ti}}{1-c_b^{\rm Ti}}\frac{P_{\rm Ar}^r Y_{\rm Ti}^{\rm Ar} + P_{\rm N_2}^r Y_{\rm Ti}^{\rm N_2^+}}{P_{\rm Ar}^r Y_{\rm Cu}^{\rm Ar} + P_{\rm N_2}^r Y_{\rm Cu}^{\rm N_2^+}}\times \\ \times\left[1 - \left(R_{\rm Ar}P_{\rm Ar}^r\frac{Y_{\rm Ti}^{r\rm Ar}}{Y_{\rm Cu}^{r\rm Ar}} + R_{\rm N}P_{\rm N_2}^r\frac{Y_{\rm Ti}^{r\rm N}}{Y_{\rm Cu}^{r\rm N}}\right)\frac{A^s}{A^t}\right],\end{aligned} \tag{7}$$

Table 1. Material-dependent parameters for Ti and Cu target atoms bombarded by atomic nitrogen and argon ions [11]

Incident ion or atom	Target atom	λ	q	μ	$E_{\rm th}$ (eV)	$E_{\rm sb}$ (eV)
N^+	Ti	0.2321	1.8168	2.0297	16.5403	4.89
N^+	Cu	0.1595	3.4102	2.1567	15.6557	3.52
Ar^+	Ti	0.3152	4.8957	1.8291	25.019	4.89
Ar^+	Cu	1.9417	14.8712	2.3907	12.9166	3.52

where c_b^{Ti} is the Ti concentration on the target surface; Y_i^j is the sputtering yield of the i-th atom due to the j-th species, i = Ti, Cu and $j = \mathrm{N}_2^+$, Ar^+, reflected N and Ar neutrals (rN and rAr). R_j and P_j^i denote the reflection coefficient and the partial pressure of the j-th species. Here, we suppose that the N_2^+ ion bombardment acts in the same way as two separate N^+ ions. The second and third terms are the re-sputtering contributions of altering the chemical composition due to the reflected N and Ar neutrals.

2.2.4. Transport of particles through the gas phase

As sputtered Ti and Cu and reflected N and Ar travel from the target to the substrate, collisions with the background N_2 gas cause the energy of these superthermal species to reduce. Because of the collisions with the background gas, the deposited energy of sputtered Ti, Cu atoms and the reflected neutrals decays exponentially with pressure-distance products as

$$\overline{E_f} = \overline{E_i} \exp\left(-\mu_m \eta \frac{Pd}{k_{\mathrm{B}} T}\right). \tag{8}$$

where η is the collision cross-section for the momentum transfer (exchange) between the sputtered particles or reflected neutrals and the background gas [3], μ_m is related to the mass ratio ($M = M_g/M_t$) and is given by [3]

$$\mu_m = 1 - \left\{\frac{|1-M|^2}{2M}\right\} \mathrm{Ln}\left\{\frac{(1+M)}{|1-M|}\right\}. \tag{9}$$

The collision cross-section η is dependent on the energy and physical properties of particles involving collisions, i.e. the radius and the mass. The collision cross-section can be approximated by an empirical power law [3]

$$\eta(E) = \eta(E_0)\left(\frac{E}{E_0}\right)^{-0.29}, \tag{10}$$

where $E_0 = 1$ eV and $\eta(E_0) = \pi(r + r_{\mathrm{quasi}})^2 \left(1 + \frac{M_s}{M_g}\right)^{1/2}$, s = reflected N and Ar neutrals, Ti and Cu; r_{quasi} is the radius of a hard spherical quasiparticle that occupies the same lateral area as N_2 molecule, and $r_{\mathrm{quasi}} = (\frac{4}{\pi})^{1/2} r_{\mathrm{cov}}$, r_{cov} is the covalent radius of the N atom (0.075 nm).

It is assumed that the energy distribution of sputtered particles $f(E)$ is [3]

$$f(E_{\mathrm{in}}, E)dE \propto$$

$$\propto dE \frac{E}{(E+E_{\mathrm{sb}})^{2.5}} \mathrm{Ln}\left(\frac{\gamma E_{\mathrm{in}}}{E+E_{\mathrm{sb}}}\right) \quad \text{for} \quad \mathrm{N}_2^+ \tag{11}$$

and

$$f(E)dE \propto dE \frac{1-\sqrt{(E_{\mathrm{sb}}+E)/\gamma E_{\mathrm{in}}}}{E^2(1+E_{\mathrm{sb}}/E)}, \quad \text{for} \quad \mathrm{Ar}^+, \tag{12}$$

where E_{in} and γ are the initial incident ion energy and the energy transfer factor from collision theory. The average initial energy $\overline{E_{ki}}$ of sputtered is determined as

$$\overline{E}_{ki} = \frac{\int\limits_0^{E_{\max}} E f(E) dE}{\int\limits_0^{E_{\max}} f(E) dE}, \tag{13}$$

where maximal energy is sometimes taken from the relation $E_{\max} = \gamma E_{\mathrm{in}} - E_{\mathrm{sb}}$ and $\gamma = 4M_g M_t/(M_g+M_t)^2$. During the transport, $\overline{E}_{ki}$ is degraded due to collisions with the gas to $\overline{E}_{kf}$, according to Eq. (8).

The throw-distance (TD) or pressure-distance characteristic is expressed as

$$\mathrm{TD} = (PL)_0 = \frac{k_{\mathrm{B}}}{\eta(E)}\left(\frac{1}{3}T_s + \frac{2}{3}T_c\right). \tag{14}$$

where T_c and T_s are the substrate and cathode temperatures, respectively. The transport factor (TF) is introduced as

$$\mathrm{TF} \propto \left|\overline{E}_{ki} - \overline{E}_{kf}\right| \mathrm{TD}. \tag{15}$$

In order to include the effect of the mass transport mechanism on the composition, the atomic Ti:Cu ratio (7) must be multiplied by the ratio of the titanium TF to that of copper (Ti:Cu TF).

3. Results and Discussion

3.1. Plasma surface interaction

Species of plasma act on the target surface through a number of collisional processes. The energy of the neutral molecular or atomic nitrogen does not allow any surface penetration, so that only the adsorption is considered for these species. Any incorporation of inert gas neutrals is neglected. It should be noted that molecular ions split into two atoms with half-energy when impinging the target surface.

The subsurface depth, on which the ion bombardment act, can be estimated by the range distribution

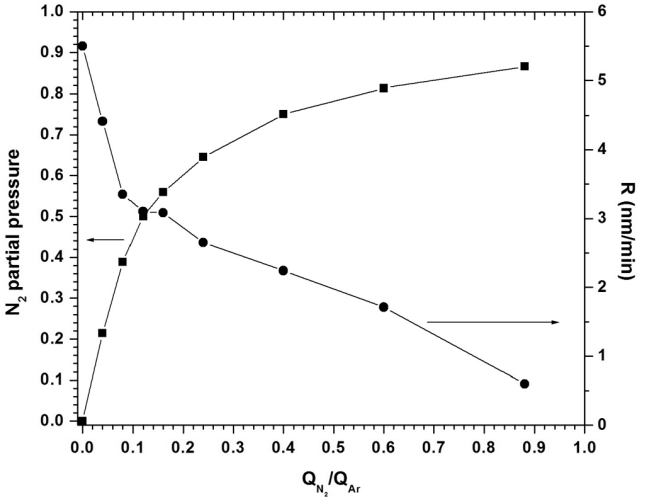

Fig. 1. Evolution of the nitrided Ti–Cu film's deposition rate and the nitrogen partial pressure ratio vs the nitrogen flow ratio

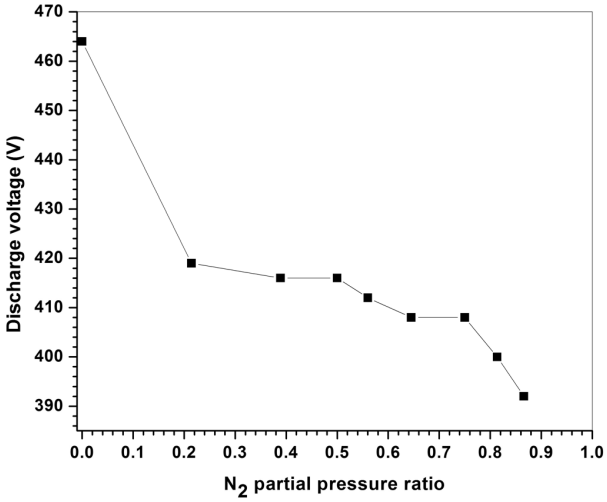

Fig. 2. Discharge voltage vs the nitrogen partial pressure ratio

of the involved ions as obtained from a static binary collision simulation using the Monte Carlo TRIM (version 2006). The mean projected ranges are around 0.8, 0.8, and 1.2 nm for Ar^+, N_2^+, and N^+ ions, respectively.

Due to the above atomic processes, an initially pure metallic target surface becomes nitrided (poisoned), as the fluence of the bombarding particles increases. At a sufficiently large fluence, a dynamic stationary state evolves with constant subsurface nitrogen profile, which is given by the balance of the nitrogen removal by surface sputtering and the nitrogen injection by ion implantation and combined adsorption.

The particle reflection coefficient is defined as a fraction of the impinging ion flux on a target that reflected. It is estimated using TRIM around 0.06, 0.22, and 0.21 for Ar^+, N_2^+, and N^+ ions, respectively.

3.2. N_2 partial pressure and deposition rate

The nitrogen partial pressure and the deposition rate plotted vs the nitrogen flow rate (Fig. 1) are representative of the reactivity of nitrogen with the Ti component of the $Ti_{13}Cu_{87}$ metalloid target, because of a low reactivity of Cu with nitrogen. As N_2 flow ratio increases to 0.12, N_2 partial pressure increases close to a linear behavior. But, for N_2 flow ratio more than 0.12, the N_2 partial pressure represents the under linear and smooth increase due to a significant getter on the target surface. Moreover, the deposition rate indicates a catastrophic poisoning of the target. The sharp decrease of the deposition rate should be related either to the poisoning of the target by a growing fraction of the reaction product or to the increasing contribution of sputtering by nitrogen, which is less efficient than argon.

3.3. Discharge characteristic

Figure 2 shows a variation in the target potential vs the nitrogen pressure ratio, when the $Ti_{13}Cu_{87}$ bicomponent target is sputtered in a constant power mode of 200 W. The absolute value of the target potential decreases, as the nitrogen pressure increases. This is generally attributed to the compound formation at the target surface and an increase of the ion-induced secondary electron emission yield (γ_{ISEE}). Here, γ_{ISEE} from the nitrided target surface is more than that from an unnitrided multicomponent target surface. The discharge current is $I = I_i(1+\gamma_{\mathrm{ISEE}})$, where I_i is the ionic current.

3.4. Chemical composition

The atomic concentration of Ti (Cu) in deposited films is generally lower (higher) than that of the original $Ti_{13}Cu_{87}$ target. It is known that the sputtering yield of Ti is less than that of Cu [14]. Also, when Ti is sputtered in an Ar/N_2 gas mixture, the sputtering yield is decreased, because a part of Ti on the target surface is nitrided. This effect is weaker for Cu, because it is more difficult to Cu nitride than Ti one due to a weaker Cu–N bonding. After being sputtered for some time, the Ti:Cu ratio on the target surface will reach equilibrium, so that the ratio of the sputtered yield of the two materials equals their ratio in the bulk target. Thus, it is like that the difference between the compositions in the target and the film is caused by their different throw

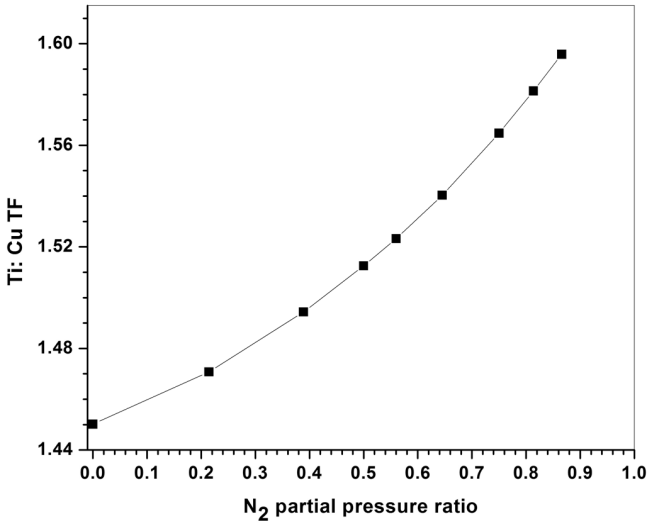

Fig. 3. Ratio of Ti to Cu transport factors (Ti:Cu TF) vs the nitrogen partial pressure ratio

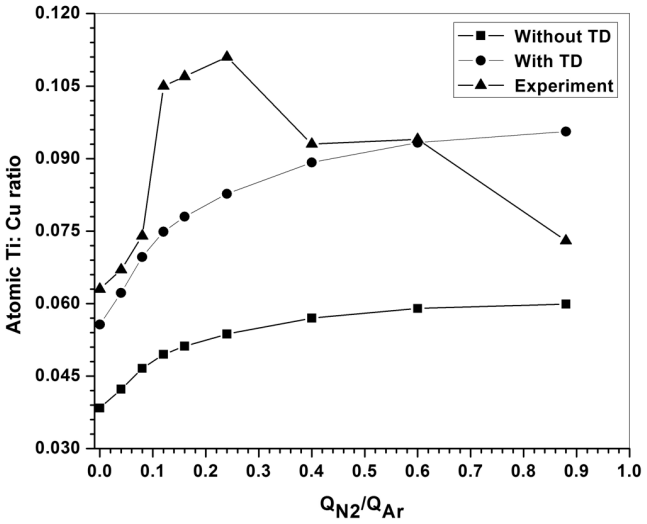

Fig. 4. Simulated and experimental values of atomic Ti:Cu ratio vs the nitrogen flow ratio

distances and the different absorption rates on the film surface.

3.5. *Determination of atomic Ti:Cu ratio using sputtering and mass transport consideration*

The atomic Ti:Cu transport factor is depicted in Fig. 3 and increases, as the nitrogen partial pressure ratio increases due to a lower scattering from nitrogen species than that of argon species in plasma during the mass transport between the target and the substrate.

Rahmati *et al.* [14–16] deposited Ti:Cu_3N thin films using the reactive DC magnetron sputtering from a $Ti_{13}Cu_{87}$ target and found that the atomic Ti:Cu ratio in as-deposited thin films (≈ 0.07) was less than that of the original target (≈ 0.15). Also, they indicated a good agreement between experimental results and the values calculated using the sputtering yield of each element from the alloyed target.

Zhao *et al.* [17] prepared Ti–Cu–N thin films using the pulsed biased arc ion plating from $Cu_{12}Ti_{88}$ and saw that the content of Cu appeared to be ≤ 4.5 at.%.

The experimental and simulated atomic Ti:Cu ratios are plotted in Fig. 4. The simulated values with throw distance (TD) consideration show a good agreement with experimental values except at moderate and high pressures. To reconcile the simulation results with experiment, the complexity of the dynamical behavior (compound formation and its removal) of the target surface should be included in the two latter pressure regions.

T a b l e 2. Atomic and molecular species taking part in surface interaction at the target, with their approximate incident energies and the corresponding interaction processes

Species	Approx. energy	Processes
N_2	30 meV	Adsorption
N	30 meV	Adsorption
N_2^+	$0.75eV_d/2$ (two N atoms)	Implantation, Reflection and sputtering
N^+	$0.75eV_d$	Implantation, Reflection and sputtering
Ar^+	$0.75eV_d$	Implantation, Reflection and sputtering

4. Conclusion

In this study, the pressure-dependent variation of a $Ti_{13}Cu_{87}$ target mode was investigated by measuring the

T a b l e 3. Nitrogen and argon flowmetre, atomic Ti and Cu concentration and films' mass

Q_{N_2}:Q_{Ar} (sccm)	Ti (%)	Cu (%)	Film mass (10^{-5} g)
0:25	5.93	94.07	60
1:25	6.32	93.68	50
2:25	6.89	93.11	39.86
3:25	9.51	90.49	39.17
4:25	9.65	90.35	41.5
6:25	9.98	90.02	39.5
10:25	8.52	91.48	39
15:25	8.57	91.43	33.33
22:25	6.85	93.15	39.17

N_2 partial pressure, deposition rate, target voltage, and Ti and Cu concentrations for various reactive N_2 gas flow ratios.

The deposition rate is reduced due to a lower sputtering yield and a higher scattering under the mass transport between the target and the substrate. Secondary electron emission yield from the nitrided target surface is greater than that for an unnitrided target surface. Therefore, at a constant sputtering power, the target voltage decreases, as the N_2 partial pressure increases.

By means of the TRIM.SP Monte-Carlo simulation, the particle reflection coefficients of reflected neutrals are calculated. The initial energies of reflected neutrals and sputtered particles at the substrate are estimated using a simple binary collision model and the distribution-weighted averages, respectively. Their final energies depend on the energy dissipation during the mass transport through the gas phase. Energy and angular characteristics of the sputtering yield were extracted from the available literature to obtain a prediction about the final composition of films. The simulated atomic Ti:Cu ratio shows the underestimated value of experimental atomic Ti:Cu ratio.

The authors would like to acknowledge financial support of Iranian nanotechnology initiative. Also, A.R. is grateful to Faculty of Physics, University of Tabriz.

1. W.D. Westwood, in *Sputter Deposition* (AVS, New York, 2003), Chap. 9.

2. K. Wasa, M. Kitabatake, and H. Adachi, *Thin Film Materials Technology* (Williams Andrew, Norwich, 2004).

3. *Reactive Sputter Deposition*, edited by D. Depla and S. Mahien (Springer, Berlin, 2008).

4. N. Malkomes and M.J. Vergohl, Appl. Phys. **89**, 732 (2001).

5. S. Ohno, D. Sato, M. Kon, P.K. Song, M. Yoshikawa, and K. Suzuki, Thin Solid Films **445**, 207 (2003).

6. E. Kusano and A. Kinbara, Thin Solid Films **281–282**, 423 (1996).

7. T. Kubart, O. Kapperttz, T. Nyberg, and S. Berg, Thin Solid Films **515**, 421 (2006).

8. The Stopping and Range of Ions in Matter, available at http://www.srim.org/.

9. Z. Wang, S.A. Cohen, D.N. Ruzic, and M.J. Goeckner, Phys. Rev. E **61**, 1904 (2000).

10. S. Mahieu and D. Depla, J. Phys. D: Appl. Phys. **42**, 053002 (2009).

11. R. Behrisch and W. Eckstein, *Sputtering by Particle Bombardment, Experiments and Computer Calculations from Threshold to MeV Energies* (Springer, Berlin, 2007).

12. Y. Yamamura, T. Takiguchi, and M. Ishida, Radiat. Eff. Def. Sol. **118**, 237 (1991).

13. A. Palmero, H. Rudolph, and F.H.P.M. Habrakan, Appl. Phys. Lett. **89**, 211501 (2006).

14. A. Rahmati, Vacuum **85**, 853 (2011).

15. A. Rahmati, H. Bidadi, K. Ahmadi, and F. Hadian, Plasma Sci. Techn. **12**, No. 6, 1 (2010).

16. A. Rahmati, H. Bidadi, K. Ahmadi, and F. Hadian, J. Coat. Tech. Res. **8**, 289 (2011).

17. Y. Zhao, X. Wang, J.Q. Xiao, B. Yu, and F. Li, Appl. Surf. Sci. **258**, 370 (2011).

Received 05.07.11

ВПЛИВ ПАРЦІАЛЬНОГО ТИСКУ АЗОТУ НА РЕАКТИВНЕ МАГНЕТРОННЕ РОЗПИЛЕННЯ $Ti_{13}Cu_{87}$ МІШЕНІ: МОДЕЛЮВАННЯ ХІМІЧНОГО СКЛАДУ

А. Рахматі, М. Ханзаде

Р е з ю м е

Мішень із спеченого композиту $Ti_{13}Cu_{87}$ було реактивно розпорошено в $Ar–N_2$ атмосфері, і розпорошену речовину осаджено на Si(111) підкладки. Досліджено залежну від тиску зміну режиму розпилення для $Ti_{13}Cu_{87}–N_2$ системи шляхом вимірювання парціального тиску N_2, швидкості осадження, напруги на мішені і концентрацій Ti та Cu для різних інтенсивностей реактивного газового потоку N_2. Поверхня $Ti_{13}Cu_{87}$ мішені починає азотуватися із зростанням інтенсивності потоку молекул азоту. Азотування викликано абсорбцією і впровадженням молекул азоту на поверхні $Ti_{13}Cu_{87}$ мішені. Отже, швидкість осадження зменшується завдяки зниженню виходу розпилення і більшому розсіянню при транспортуванні речовини від мішені до підкладки. Вихід вторинної електронної емісії з азотованій поверхні мішені більше, ніж без азотування. Тому за сталої потужності розпилення напруга на мішені зменшується при збільшенні парціального тиску азоту. Розраховано коефіцієнти відбиття нейтральних частинок методом TRIM.SP Монте-Карло. Початкові енергії відображених нейтральних і розпорошених частинок поблизу підкладки оцінено, відповідно, в рамках простої моделі бінарних зіткнень і з середніми зваженими з розподілом. Кінцеві енергії залежать від дисипації енергії при проходженні крізь газове середовище. Відомі з літератури дані

за енергетичними та кутовими характеристиками розпилення використано для передбачення складу плівок.

ВЛИЯНИЕ ПАРЦИАЛЬНОГО ДАВЛЕНИЯ АЗОТА НА РЕАКТИВНОЕ МАГНЕТРОННОЕ РАСПЫЛЕНИЕ $Ti_{13}Cu_{87}$ МИШЕНИ: МОДЕЛИРОВАНИЕ ХИМИЧЕСКОГО СОСТАВА

А. Рахмати, М. Ханзаде

Р е з ю м е

Мишень из спеченного композита $Ti_{13}Cu_{87}$ была реактивно распылена в $Ar–N_2$ атмосфере, и распыленное вещество осаждено на Si(111) подложки. Исследовано зависящее от давления изменение режима распыления для $Ti_{13}Cu_{87}–N_2$ системы путем измерения парциального давления N_2, скорости осаждения, напряжения на мишени и концентраций Ti и Cu для разных интенсивностей реактивного газового потока N_2. Поверхность $Ti_{13}Cu_{87}$ мишени начинает азотироваться с ростом интенсивности потока молекул азота. Азотирование вызвано абсорбцией и внедрением молекул азота на поверхности $Ti_{13}Cu_{87}$ мишени. Следовательно, скорость осаждения уменьшается благодаря понижению выхода распыления и большему рассеянию при транспорте вещества от мишени к подложке. Выход вторичной электронной эмиссии из азотированной поверхности мишени больше, чем без азотирования. Поэтому при постоянной мощности распыления напряжение на мишени уменьшается при увеличении парциального давления азота. Рассчитаны коэффициенты отражения нейтральных частиц методом TRIM.SP Монте-Карло. Начальные энергии отраженных нейтральных и распыленных частиц возле подложки оценены, соответственно, в рамках простой модели бинарных столкновений и со средними взвешенными с распределением. Конечные энергии зависят от диссипации энергии при прохождении через газовую среду. Известные из литературы данные по энергетическим и угловым характеристикам распыления использованы для предсказания состава пленок.